

AUG 27 1981

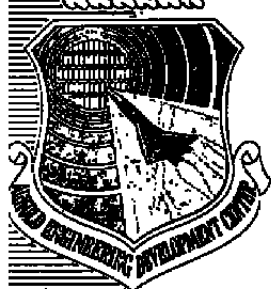
OCT 1 1981

100-03-74

MAY 29 1984

AEDC-TR-81-15

c3



Study of Impact Frequency Effects on Hypervelocity Erosion Processes

E. E. Callens, Jr., and W. R. Lawrence
ARO, Inc.

August 1981

Final Report for Period January 12, 1976 – September 30, 1978

Approved for public release; distribution unlimited.

Property of U.S. Air Force
Arnold Air Force Station
FAC000000000000000000000000000000

**ARNOLD ENGINEERING DEVELOPMENT CENTER
ARNOLD AIR FORCE STATION, TENNESSEE
AIR FORCE SYSTEMS COMMAND
UNITED STATES AIR FORCE**

NOTICES

When U. S. Government drawings, specifications, or other data are used for any purpose other than a definitely related Government procurement operation, the Government thereby incurs no responsibility nor any obligation whatsoever, and the fact that the Government may have formulated, furnished, or in any way supplied the said drawings, specifications, or other data, is not to be regarded by implication or otherwise, or in any manner licensing the holder or any other person or corporation, or conveying any rights or permission to manufacture, use, or sell any patented invention that may in any way be related thereto.

Qualified users may obtain copies of this report from the Defense Technical Information Center.

References to named commercial products in this report are not to be considered in any sense as an endorsement of the product by the United States Air Force or the Government.

This report has been reviewed by the Office of Public Affairs (PA) and is releasable to the National Technical Information Service (NTIS). At NTIS, it will be available to the general public, including foreign nations.

APPROVAL STATEMENT

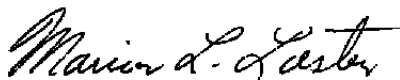
This report has been reviewed and approved.



MARSHALL K. KINGERY
Directorate of Technology
Deputy for Operations

Approved for publication:

FOR THE COMMANDER



MARION L. LASTER
Director of Technology
Deputy for Operations

UNCLASSIFIED

REPORT DOCUMENTATION PAGE		READ INSTRUCTIONS BEFORE COMPLETING FORM
1. REPORT NUMBER AEDC-TR-81-15	2. GOVT ACCESSION NO.	3. RECIPIENT'S CATALOG NUMBER
4. TITLE (and Subtitle) STUDY OF IMPACT FREQUENCY EFFECTS ON HYPERVELOCITY EROSION PROCESSES		5. TYPE OF REPORT & PERIOD COVERED Final Report - Jan. 12, 1976 to Sept. 30, 1978
		6. PERFORMING ORG. REPORT NUMBER
7. AUTHOR(s) E. E. Callens, Jr. and W. R. Lawrence, ARO, Inc., a Sverdrup Corporation Company		8. CONTRACT OR GRANT NUMBER(s)
9. PERFORMING ORGANIZATION NAME AND ADDRESS Arnold Engineering Development Center/DOT Air Force Systems Command Arnold Air Force Station, Tennessee 37389		10. PROGRAM ELEMENT, PROJECT, TASK AREA & WORK UNIT NUMBERS Program Element 65807F
11. CONTROLLING OFFICE NAME AND ADDRESS Arnold Engineering Development Center/DOS Air Force Systems Command Arnold Air Force Station, Tennessee 37389		12. REPORT DATE August 1981
14. MONITORING AGENCY NAME & ADDRESS (if different from Controlling Office)		13. NUMBER OF PAGES 20
		15. SECURITY CLASS. (of this report) UNCLASSIFIED
		15a. DECLASSIFICATION/DOWNGRADING SCHEDULE N/A
16. DISTRIBUTION STATEMENT (of this Report) Approved for public release; distribution unlimited.		
17. DISTRIBUTION STATEMENT (of the abstract entered in Block 20, if different from Report)		
18. SUPPLEMENTARY NOTES Available in Defense Technical Information Center (DTIC)		
19. KEY WORDS (Continue on reverse side if necessary and identify by block number) hypervelocity impact ranges (facilities) erosion particle collisions debris flow fields flight bow shock environment		
20. ABSTRACT (Continue on reverse side if necessary and identify by block number) Erosive particle impact frequency-dependent mechanisms are examined to determine potentially important spatial and time-dependent interactions which can influence flight and ground test erosion performance. Specific consideration is given to the interaction of incident erosive particles with impact-generated ejecta and to the shielding effect which this interaction can have on the observed material erosion characteristics. It is		

UNCLASSIFIED

20. ABSTRACT (Continued)

concluded that debris shielding does not occur to any significant degree in the real flight environment, but could be a potential problem in correlating high concentration range/track test results.

PREFACE

The research described herein was conducted by the Arnold Engineering Development Center (AEDC), Air Force Systems Command (AFSC), and Mr. M. K. Kingery was the Air Force project manager. The results were obtained by ARO, Inc., AEDC Group (a Sverdrup Corporation Company), operating contractor for the AEDC, AFSC, Arnold Air Force Station, Tennessee. The results reported include those obtained under ARO Projects Nos. V43G-14A (FY76), V43G-19A (FY77 and FY77), and V32S-P7A (FY78). The data analysis was completed on September 30, 1978, and the manuscript was submitted for publication on November 19, 1979.

Messrs. Callens and Lawrence are currently employed by Calspan Field Services, Inc., AEDC Division.

CONTENTS

	<u>Page</u>
1.0 INTRODUCTION	5
2.0 ANALYSIS OF IMPACT FREQUENCY EFFECTS	5
2.1 Analysis of Available Experimental Data	7
2.2 Debris-Shielding Model Development	10
3.0 SUMMARY	17
REFERENCES	18

ILLUSTRATIONS

Figure

1. Impact-Generated Debris Cloud Development	7
2. Debris Leading-Edge Velocity as a Function of Erosive Particle Diameter for Impact Velocities of 8,000 and 12,000 fps	8
3. Debris Behavior Subsequent to Plume Arrival at Bow Shock	9
4. Computed Trajectory of a Graphite Debris Particle within the Flow Field of a Typical Track K Model	12
5. Schematic Diagram of Debris Buildup within an Erosive Field of Length l_f	15
NOMENCLATURE	19

1.0 INTRODUCTION

Reentry vehicle material erosion resulting from repetitive impacts of hypervelocity environmental particles is a complex phenomenon involving interactions between the impacting particles, the aerothermal fluid environment surrounding the vehicle, the vehicle material, and the debris fragments generated by particle impacts upon the vehicle surface. First-order estimates of potential impact-induced damage to reentry vehicle nosetip and heat shield material are often derived from simple, single particle-surface interactions in the absence of flow-field and debris interactions. The adequacy of this approach obviously depends on the relative magnitude of the possible interactions under various conditions of vehicle velocity and particle concentration. In this report, consideration is given to the nature and potential extent of these interactions from the point of view of deriving first-order estimates of the magnitude of various impact frequency effects.

2.0 ANALYSIS OF IMPACT FREQUENCY EFFECTS

The frequency of particle impacts near the stagnation region of a vehicle traversing a 5×10^{-7} gm/cm³ cloud of 200- μ m-diam water droplets at 3,000 m/sec is about 3.6×10^4 impacts/sec-cm². Under these conditions, two classes of interactions can be important — (1) those attributed to spatial and (2) those due to time-dependent events. Overlapping of impact craters generated at significantly different times represents a spatial interaction, whereas successive encounters of two particles within the time interval of crater formation or ejecta debris removal represents a potential time-dependent interaction mechanism. A number of mechanisms can be postulated whereby potentially important spatial and time-dependent interactions can be generated. These include the following:

1. Particle impact upon previously damaged surface material,
2. Particle distortion and/or breakup within vehicle flow field,
3. Disturbance of the flow field attributed either to incident particles or impact ejecta,
4. Aerothermal ablation of surface material, and
5. Ejecta material interactions with incident particles, resulting in a shielding effect.

Since the relative importance of these and other mechanisms may vary depending on vehicle velocity and environmental conditions, it is important to understand the physical processes whereby these mechanisms are generated in order that appropriate models of these

events can be formulated for engineering design consideration. In addition, proper formulation and evaluation of ground test facility experiments depend upon an understanding of the complex physical processes which can interact to influence the nature of results obtained.

Analyses of several aspects of the ablation/erosion phenomena have been conducted during the past several years (e.g., Ref. 1), and understanding the nature of the process has been improved. However, understanding the erosion process under conditions of high impact frequency, where coupling between discrete impact events can be of major importance, is still incomplete. Attempts to develop general correlation parameters for conditions where these complex mechanisms are operative have not been successful. In the present analysis, consideration is given to the interaction of incident erosive particles with impact-generated ejecta and to the shielding effect which this interaction can have on the observed material erosion characteristics. An attempt is made to formulate an appropriate debris-shielding mathematical model on the basis of relevant experimentally observed characteristics of the process.

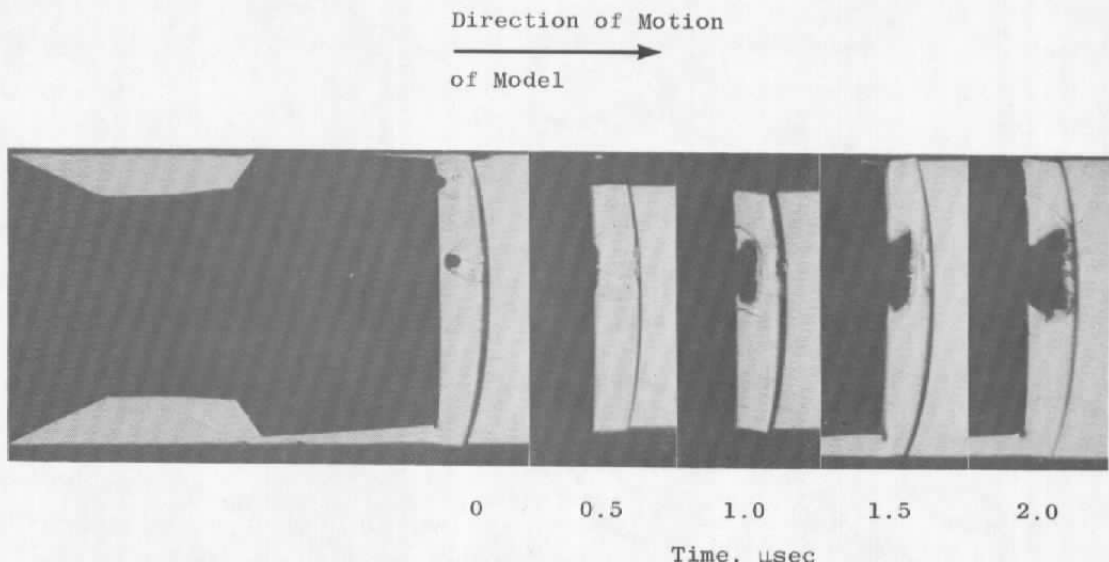
In this analysis, consideration is given to (1) physical processes for erosion under conditions of high impact frequency, and (2) development and evaluation of a specific erosion prediction model. The approach taken was as follows:

1. An examination of available single-impact photographic data was made to determine the nature of the debris behavior subsequent to the hypervelocity impact event.
2. Available numerical results for impact crater growth and ejecta formation were examined to provide estimates for debris particle initial conditions within the vehicle shock layer.
3. A numerical computation code was developed to investigate the dynamics of debris particle behavior within the vehicle nosetip flow field. The results of these calculations were used to provide estimates of particle density distribution ahead of the nosetip.
4. A simple mathematical model for incoming erosive particle slowdown within the multiphase environment generated by the debris mass distribution was constructed to estimate the shielding potential of this debris cloud.

The following discussion summarizes the above efforts and includes a discussion of results obtained by application of the approach to a representative example.

2.1 ANALYSIS OF AVAILABLE EXPERIMENTAL DATA

An examination was made of experimental single-impact debris behavior obtained during recent erosion tests at the Arnold Engineering Development Center (AEDC). The development of a representative debris cloud generated by the impact of a free-falling 1,150- μm -diam water droplet upon an ATJ-S graphite nosetip moving at a velocity of approximately 12,000 fps relative to the droplet is shown in Fig. 1, obtained using the sequential five-frame laser system of the AEDC Range K. The ambient range pressure for this show was 348 torr, and the time between photographs was approximately 0.5 μsec . The leading edge of the debris cloud appears to move at a velocity of 6,100 fps relative to the nosetip surface.



Particle Type - Water
 Particle Diameter = 1,150 μm
 Impact Velocity = 12,000 fps
 Free-Stream Pressure = 348 torr
 Nosetip Material - ATJ-S Graphite
 Time between Photographs = 0.5 μsec

Figure 1. Impact-generated debris cloud development.

Measurements of debris cloud leading-edge velocity (relative to nosetip surface) as a function of water droplet diameter for impact velocities of 8,000 to 12,000 fps are shown in

Fig. 2. The nosetip material used for these shots is ATJ-S graphite. The cloud leading-edge velocity increases with increasing erosive particle diameter.

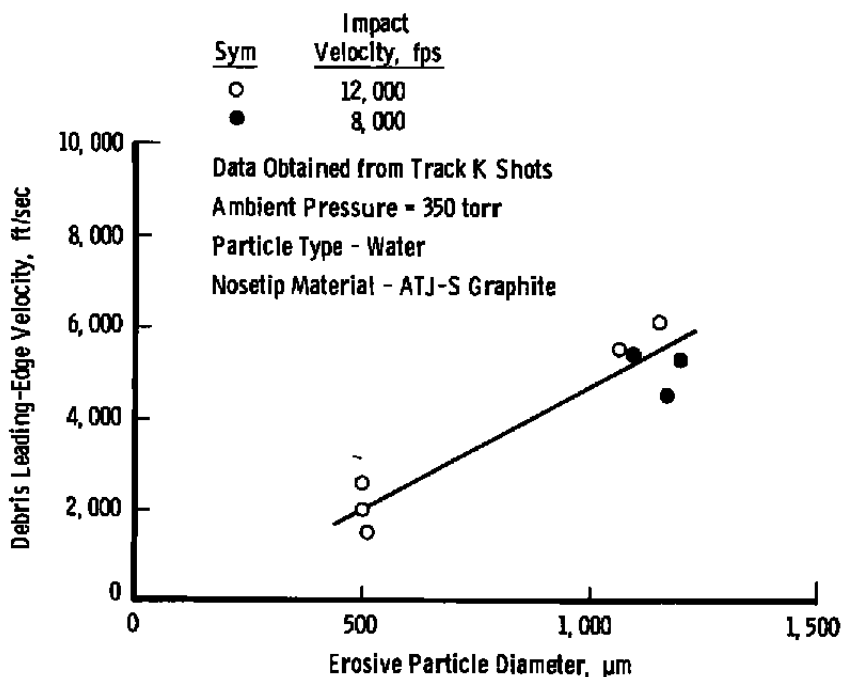
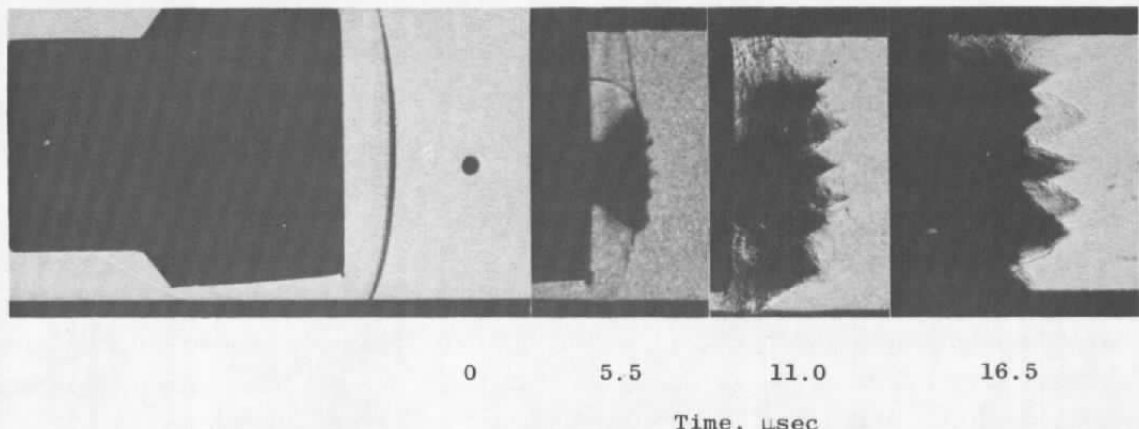


Figure 2. Debris leading-edge velocity as a function of erosive particle diameter for impact velocities of 8,000 and 12,000 fps.

Typical experimental debris behavior observed subsequent to plume arrival at the bow shock is shown in Fig. 3. The photographic results were obtained with the five-frame sequential laser system on shot 3,079 in Range K (only first four frames were usable). The debris is generated by the impact of a 1,500- μm -diam water droplet at a velocity of 11,800 fps relative to the GE 223 nosetip material, and the time interval between successive frames is approximately 5.5 μsec . Subsequent to plume arrival at the shock, a dispersal of the plume debris begins as the debris particle behavior becomes dominated by the flow field surrounding the impacted nosetip. At 11 μsec after shock arrival, the debris has not only continued upstream of the original bow shock location but has filled most of the visible area between the upper and lower edges of the nosetip. The bow shock has been replaced by several oblique shocks generated by debris particles penetrating the free stream ahead of the bow shock. During the 16.5 μsec between frame one and frame four of the sequence shown, the nose has traveled approximately 0.195 feet.



Particle - 1,500- μ m-diam Water
 Nosetip Material - GE 223 Carbon-Carbon Composite
 Impact Velocity = 11,800 fps
 Time between Photographs = 5.5 μ sec

Figure 3. Debris behavior subsequent to plume arrival at bow shock.

An analysis of the available Track K experimental results indicates the following:

1. As a result of single-particle hypervelocity impact on typical reentry vehicle nosetip materials, significant debris is ejected into the flow field surrounding the nosetip;
2. The residence time of debris particles within the region of the nosetip can be longer than the time required to form the crater itself; and
3. The late-time behavior of the debris particles is dominated by the vehicle flow field, which can itself be significantly influenced and altered by the mutual interaction.

However, in these analyses we were not able to determine the following:

1. The distribution of debris particle sizes,
2. The ejection velocities of the various particles during the crater forming phase,
3. The debris mass density distribution throughout the flow field as a function of time after impact, and
4. The time required for complete removal of debris from the flow field.

2.2 DEBRIS-SHIELDING MODEL DEVELOPMENT

Experiments conducted in various ground test facilities have shown that the erosion-induced mass removal ratio decreases as the erosive field mass concentration increases (e.g., Ref. 2). A possible explanation of this effect is that there is incoming particle slowdown and/or breakup resulting from interaction with debris ejecta generated by earlier particle impacts with the surface. To estimate the magnitude of this effect, it is necessary to determine (1) the nature and characteristics of the debris ejecta and (2) the influence of its interaction both with the vehicle flow field and with incoming erosive particles. The phenomenon is thus quite complex, although several aspects of the process can be addressed separately to first order. That is, consideration can be given to the following:

1. Characteristics of impact crater and ejecta formation, including debris velocity and duration of the event;
2. Influence of vehicle flow field on ejecta material, leading primarily to an estimate of the debris residence time in the shock layer ahead of the vehicle surface; and
3. Modification of incoming particles caused by multiple impacts with debris material within the vehicle flow field.

Item 1 is addressed on the basis of available numerical code calculations (Ref. 3) for hypervelocity particle impacts into graphite; item 2 is addressed on the basis of a numerical code developed under this study to determine uncoupled, single debris particle dynamics within a specified flow field; and item 3 is addressed on the basis of a simplified analytical debris encounter model also developed as part of this effort. A study of available debris photographs made using the five-frame laser system in Track K provided the experimental observations upon which the numerical and analytical development work is based. Since the majority of these data were derived from shots made at velocities near 10,000 fps, this velocity was chosen for the representative example to be discussed later.

2.2.1 Characteristics of Crater Growth and Ejecta Formation

The problem of interest here is that of an impact between a liquid (e.g., water) or solid (e.g., silica) particle (diameter of the order of 10 to 1,000 μm) and a brittle material such as graphite. Although predictably different in many respects, impacts by liquid and solid particles exhibit grossly similar features overall. For a 1,000- μm -diam water droplet impacting a graphite surface at 10,000 and 20,000 fps, the corresponding crater formation completion times are 6 and 8 μsec , respectively (Ref. 3). During this formation period,

material is ejected from the crater, and after penetrating some distance upstream into the oncoming flow this material is swept downrange by the flow past the body. This residence time can be many times the basic crater formation time and depends on such parameters as debris particle size, ejecta velocity, and nature of particle-flow-field interaction. For the 1,000- μ m, 10,000-fps impact case, it can be shown theoretically (Ref. 3) that the ejecta material leaves the crater with velocities which vary with time after impact as follows:

Time after Impact, μ sec	Ejecta Velocity, ft/sec
0.7	3,000
4.1	800
6.0	0

For these conditions, the theoretical calculations predict a debris plume leading edge moving normal to the surface at a constant rate of approximately 3,000 fps after 3 μ sec. These calculations do not include any effect resulting from debris particle interaction with the surrounding environment, however.

An analysis of high-speed photographs of the impact process appears to indicate that the ejected material particles are considerably smaller than the corresponding impact particles (Fig. 1). Presumably, a variety of particle sizes are ejected, with larger peripheral crater fragments ejected in the later development phase and with smaller, nearly vaporous, material ejected initially. If the initial velocity of this material can be measured, an estimate of its size can be obtained from measurement of the forward penetration of this debris against the oncoming flow forward of the nosetip. Some of these comparisons are discussed later.

2.2.2 Dynamics of Debris Particles within Vehicle Flow Field

In order to estimate the debris cloud mass density at any given time, the equations describing the dynamics of a single debris particle as influenced by the vehicle nosetip flow field were solved using an uncoupled interaction model whereby a prescribed flow field results in debris particle acceleration and removal from the nosetip region. The interaction is defined in terms of a particle drag coefficient which can, in general, be a function of the local relative Mach number and Reynolds number which the particle experiences at any given point within or outside the nosetip shock layer. Initial conditions for the debris particle are prescribed at the material surface where the cratering and mass ejection phenomena

occur. Solutions can be obtained for several sets of initial conditions (corresponding to various phases of crater formation and debris ejection, as discussed earlier) and accumulated to provide a mosaic of the entire debris cloud characteristics, including equivalent debris cloud density as a function of time after crater formation.

The flow field about the vehicle nosetip is taken to be that described by the program of Ref. 4, which presents a calculation procedure for determining the axisymmetric supersonic flow past blunt bodies with sonic corners. In this program, numerical solutions are derived using the system of equations given by the one-strip method of Belotserkovskii (Ref. 5). The flow-field properties of interest are the surface pressure, shape and location of the detached bow shock wave, and the velocity distribution in the flow region between the shock and body surface.

An example calculation of the trajectory of a 65- μm -diam graphite debris particle within the flowfield of a 0.75-in.-diam nosetip traveling at 10,000 fps at an ambient pressure of 350 torr is shown in Fig. 4. The initial velocity (magnitude and direction) of the debris at its origin (debris generating crater) is 800 fps at 30 deg relative to the flight direction. The debris particle forward velocity is reduced to zero shortly after the particle penetrates the bow shock, at approximately 13 μsec , and subsequently impacts the nosetip surface at 38 μsec . During the 38 μsec that the debris particle is located ahead of the nosetip surface, the possibility exists for it to interact with an incoming erosive particle. During this time, the

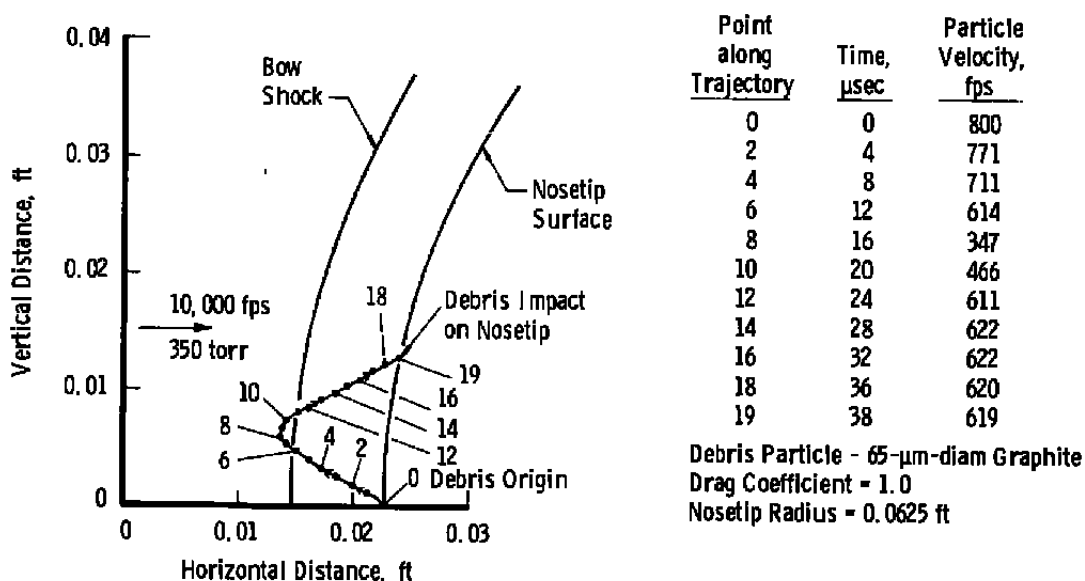


Figure 4. Computed trajectory of a graphite debris particle within the flow field of a typical Track K model.

nose tip can travel a distance of approximately 4.6 inches. If additional erosive particles are encountered within this distance (as would be expected for locally heavy erosive particle concentrations), it can be assumed that accumulated-debris interaction with these particles will alter the nose tip surface damage resulting from subsequent impacts by these particles. The nature of the interaction is addressed in the following section. For purposes of this study, this interaction is assumed to result only in a slowdown (relative to the nose tip surface) of the incoming erosive particle.

2.2.3 Hypervelocity Particle Slowdown in a Multiphase Environment

The task is to estimate the reduction in particle velocity relative to an approaching surface as a result of interaction with a debris layer (having a thickness of the order of the shock layer thickness). This interaction has been modeled as a series of discrete impacts between a large incoming particle and many smaller debris particles, the net result of which is a deceleration of the larger particle. Measurements of momentum transfer to a large target, as a result of hypervelocity impact from a smaller particle, indicate that the process is more nearly represented by elastic collision results (caused by debris ejection) rather than by inelastic collision results even though the impacting particle is completely destroyed by the impact process.*

Considering the elastic collision of two particles having very different masses gives the results outlined below. Before collision the larger particle, having mass M and velocity u_0 relative to the smaller particle having mass m_i , has momentum Mu_0 . For perfectly elastic collisions, the momentum change of the larger particle will be

$$\Delta(Mu) = -2(m_i)u_0 \quad (1)$$

or

$$\frac{\Delta u}{u_0} = -2 \frac{m_i}{M} \quad (2)$$

The net change in velocity of the larger particle after encountering many particles having masses Δm will be

$$\sum_i \frac{\Delta u}{u} = -\frac{2}{M} \sum_i m_i \quad (3)$$

*Unpublished data obtained during calibration of ballistic pendulum design in the AEDC von Karman Gas Dynamics Facility Range K, 1978.

so that

$$u = u_0 e^{-\frac{2}{M} \sum m_i} \quad (4)$$

This equation relates the incident particle slowdown to the accumulated encountered debris mass, $\sum m_i$. For example, should an incoming 100- μm -diam (1.5 μgm) silica particle encounter only one percent of the debris mass generated by a previous surface impact of a like particle traveling at 10,000 fps (assuming a mass removal ratio of 25), the resulting particle velocity will be 6,100 fps. However, determination of the number of debris particle impacts resulting from multiple previous erosive particle impacts upon the nosetip surface presents a formidable computational challenge. A simplified analytical result can be obtained by recasting the interaction model to one based on an effective particle drag coefficient within the multiphase (gas and debris) environment generated by impact debris. The drag coefficient can be determined from experimental data.

In traversing a distance δ through a debris layer having a density σ , a particle of radius r and mass m will slow down according to

$$m \frac{du}{dt} = -\frac{1}{2} \sigma u_{\text{rel}}^2 \pi r^2 C_{D_{\text{eff}}} \quad (5)$$

If the relative velocity between the particle and multiphase environment, u_{rel} , is taken to be approximately the same as u , then this equation can be integrated to give

$$\frac{u_{\text{final}}}{u_0} = e^{-\beta \delta} \quad (6)$$

where u_0 is initial velocity of the particle relative to the surface, u_{final} is the impact velocity as a result of traversing the debris layer, and

$$\beta = \frac{\sigma \pi r^2 C_{D_{\text{eff}}}}{2m} \quad (7)$$

Assuming that all of the debris generated by a given number of impacts remains in front of the model nosetip having frontal area πR^2 , then the mass of material within the debris layer, \tilde{M} , is (see Fig. 5)

$$\tilde{M}(x_1) = \int_{x=0}^{x_1} \tilde{G}(x) \pi R^2 c_s dx \quad (8)$$

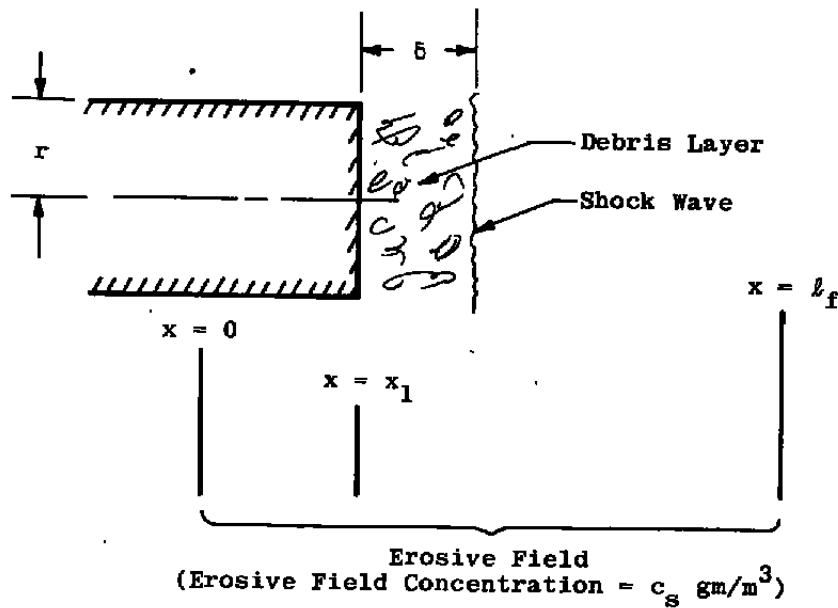


Figure 5. Schematic diagram of debris buildup within an erosive field of length l_f .

where $\tilde{G}(x)$ is the local mass removal ratio (mass removed divided by mass impacted), which is a function of distance flown within the erosive field, x . At the beginning of the erosive field, $\tilde{G}(0) = G_0$, the mass removal ratio in the absence of debris-shielding effects. The multiphase material density ahead of the nosetip is approximately that attributed to debris material alone and is given by

$$\sigma = \frac{\tilde{M}(x_1)}{\pi R^2 \delta} = \frac{c_s}{\delta} \int_{x=0}^{x_1} \tilde{G}(x) dx \quad (9)$$

The average mass removal ratio for the entire erosive field of length l_f will be

$$\bar{G}(l_f) = \frac{\tilde{M}(l_f)}{\int_{x=0}^{l_f} \pi R^2 c_s dx} \quad (10)$$

which can be shown to be

$$\bar{G}(l_f) = \frac{\int_{x=0}^{l_f} \tilde{G}(x) dx}{l_f} \quad (11)$$

Considering again the influence of the debris layer upon erosive particle slowdown and assuming an impact velocity-squared dependence of \tilde{G} , then

$$\tilde{G}(x_1) = \tilde{G}(u) = G_o \cdot \left(\frac{u_{final}}{u_o} \right)^2 \quad (12)$$

or,

$$\tilde{G}(x_1) = G_o e^{-2\beta\delta} \quad (13)$$

with $\beta = \beta(x_1)$. Thus

$$\tilde{G}(x_1) = G_o \exp(-\sigma \pi r^2 C_D \delta / m) \quad (14)$$

with

$$\sigma = \frac{c_s}{\delta} \int_{x=0}^{x_1} \tilde{G}(x) dx \quad (15)$$

Taking the logarithm of both sides of Eq. (14) and differentiating with respect to x gives

$$\frac{1}{\tilde{G}} \frac{d\tilde{G}}{dx} = -C \tilde{G} \quad (16)$$

where

$$C = \frac{c_s \pi r^2 C_D}{m}$$

This can be integrated to give

$$\frac{\tilde{G}(x_1)}{G_o} = \frac{1}{1 + \frac{G_o \pi r^2 C_D c_s x_1}{m}} \quad (17)$$

For example, for flight through an erosive environment described by the following parameters, representative of flight conditions,

$$G_0 = 27$$

$$r = 300 \mu\text{m}$$

$$C_D = 0.4 \text{ (estimated)}$$

$$c_s = 1 \text{ gm/m}^3$$

$$x_1 = 0.1 \text{ m}$$

$$m = 45 \mu\text{gm,}$$

then

$$\frac{\tilde{G}(x_1)}{G_0} = 0.99 \quad (18)$$

However, for an erosive field local concentration of 40 gm/m³ (typical of corresponding ground test discrete erosive fields), these same conditions will result in $G/G_0 = 0.79$. Hence, although debris shielding does not appear to be significant in a representative flight environment, it can be a potential problem in correlating ground test simulation results obtained using discrete concentrated erosive fields.

3.0 SUMMARY

Consideration has been given to the interaction of incident erosive particles with impact-generated ejecta and to the shielding effect which this interaction can have on the observed material erosion characteristics. First, an examination was made of experimental single-impact debris behavior obtained during recent erosion tests at AEDC. Analysis of these data indicates that (1) significant debris is ejected into the flow field surrounding the nosetip; (2) the residence time of debris particles within the region of the nosetip can be longer than the time required to form the crater itself; and (3) the late-time behavior of the debris particles is dominated by the vehicle flow field, which can itself be significantly influenced and altered by the mutual interaction. From an analysis of the available experimental data, it was not possible to determine (1) the distribution of debris particle sizes, (2) the ejection velocities of various particles during the crater forming phase, (3) the debris mass density distribution throughout the flow field as a function of time after impact, and (4) the time required for complete removal of debris from the flow field.

A numerical code was developed wherein the equations describing the dynamics of a single debris particle as influenced by the vehicle nosetip flow field are solved using an

uncoupled interaction model for a prescribed flow field. Solutions can be obtained for several sets of initial conditions (corresponding to various phases of crater formation and debris ejection) and accumulated to provide a mosaic of the entire debris cloud characteristics.

Finally, a simplified analytical formulation was developed to estimate erosion reduction based upon a debris-encounter model employing an effective drag coefficient of an erosive particle within a multiphase (debris-laden) flow-field environment.

An examination of the available experimental data and the simplified analytical and numerical results discussed herein suggests that the potential for debris-shielding effects to be experimentally important is sufficiently significant to warrant consideration of these effects during the analysis of ground test erosion data. A more definitive assessment of these effects is not possible at this time because of lack of data relative to several aspects of the problem. Specifically, additional study is needed in the following areas:

- (1) Increased understanding is needed relative to the influence of debris encounter upon an incoming erosive particle. Measurements of erosive particle slowdown as a result of interaction with particular clouds of various mass densities are needed, as are measurements of erosive particle mass loss and breakup.
- (2) The mechanism of debris interaction during multiple particle encounters, including mutual interaction effects, is required. A statistical model based on encounter probabilities may be a useful approach to the development of a model of these effects.

REFERENCES

1. Adler, W. F., ed. *Erosion: Prevention and Useful Application*. American Society for Testing and Materials, Philadelphia, PA, 1979.
2. Reinecke, W. G. "Debris Shielding during High-Speed Erosion." *AIAA Journal*, Vol. 12, No. 11, November 1974, pp 1592-1594.
3. Kreyenhagen, K. N., et al. "Direct Impact Effects in Hypersonic Erosion." SAMSO-TR-73-339, August 1973.

4. South, J. C., Jr. "Calculation of Axisymmetric Supersonic Flow Past Blunt Bodies with Sonic Corners, Including a Program Description and Listing." NASA TN D-4563, May 1978.
5. Belotserkovskii, O. M. "Flow with a Detached Shock Wave about a Symmetrical Profile." *Journal of Applied Mathematics and Mechanics*, Vol. 22, No. 2, 1958, pp. 279-296.

NOMENCLATURE

$C_{D_{ell}}$	Particle drag coefficient
c	Erosive field concentration, gm/m ³
G	Mass removal ratio (ratio of mass of material removed to mass of material encountered)
G_0	Mass removal ratio in the absence of debris-shielding effects
\tilde{G}	Local mass removal ratio within an erosive field
\bar{G}	Average G defined in Eq. (10)
l	Length of erosive field, ft
M	Large particle mass [Eq. (1)], gm
\tilde{M}	Material mass within debris layer, gm
m	Erosive particle mass, gm
m_i	Small particle mass [Eq. (1)], gm
R	Nosetip radius, m
r	Particle radius, m

t	Time, sec
u	Particle velocity, ft/sec
u_0	Particle velocity before debris field encounter, ft/sec
u_{final}	Particle velocity at impact upon nosetip surface, ft/sec
x	Distance flown, m
x_1	Distance flown within erosive field, m
β	Defined in Eq. (7)
Δ	Increment
δ	Thickness of debris layer
σ	Debris layer mass density